

DISCOVERY OF EIGHT NEW EXTREMELY METAL-POOR GALAXIES IN THE SLOAN DIGITAL SKY SURVEY

ALEXEI Y. KNIAZEV^{1,3}, EVA K. GREBEL¹, LEI HAO², MICHAEL A. STRAUSS², JONATHAN BRINKMANN⁴, MASATAKA FUKUGITA⁵kniazev@mpia.de, grebel@mpia.de,
haol@astro.princeton.edu, strauss@astro.princeton.edu,
jb@apo.nmsu.edu, fukugita@icrr.u-tokyo.ac.jp*Accepted to ApJ Letters*

ABSTRACT

We report the discovery of eight new extremely metal-poor galaxies (XMPGs; $12+\log(\text{O}/\text{H}) < 7.65$) and the recovery of four previously known or suspected XMPGs (I Zw 18, HS 0822+3542, HS 0837+4717 and A1116+517) using Sloan Digital Sky Survey (SDSS) spectroscopy. These new objects were identified after an analysis of 250,000 galaxy spectra within an area of $\sim 3000 \text{ deg}^2$ on the sky. Our oxygen abundance determinations have an accuracy of ≤ 0.1 dex and are based on the temperature-sensitive [O III] $\lambda 4363 \text{ \AA}$ line and on the direct calculation of the electron temperature. We briefly discuss a new method of oxygen abundance determinations using the [O II] $\lambda 7319, 7330 \text{ \AA}$ lines, which is particularly useful for SDSS emission-line spectra with redshifts ≤ 0.024 since the [O II] $\lambda 3727 \text{ \AA}$ emission line falls outside of the SDSS wavelength range. We detect XMPGs with redshifts ranging from 0.0005 to 0.0443 and M_g luminosities from -12^m4 to -18^m6 . Our eight new XMPGs increase the number of known metal-deficient galaxies by approximately one quarter. The estimated surface density of XMPGs is 0.004 deg^{-2} for $r \leq 17^m77$.

Subject headings: galaxies: abundances — galaxies: dwarf — galaxies: evolution

1. INTRODUCTION

Star-forming, extremely metal-poor galaxies (XMPGs) in the nearby Universe have received much attention, since some of these objects may be primeval galaxies that are now experiencing their first major burst of star formation (e.g., Searle & Sargent 1972; Izotov & Thuan 1999; Kunth & Östlin 2000). XMPGs are characterized by low nebular oxygen abundances ($12+\log(\text{O}/\text{H}) < 7.65$; e.g., Kunth & Östlin 2000, hereafter KÖ00). Although there have been a number of special emission-line surveys for XMPGs (e.g., Terlevich et al. 1991; Pustilnik et al. 1999; Salzer et al. 2000; Ugryumov et al. 2003), very few objects of this class are known. Combining measurements based on different methods from a variety of sources compiled by KÖ00 with the recent studies by van Zee (2000); Kniazev et al. (2001); Pustilnik et al. (2002); Skillman et al. (2003) and Lee et al. (2003) gives a total of ~ 30 currently known or suspected XMPGs. The majority of these galaxies are starbursting blue compact galaxies (BCGs), while the remainder are more quiescently evolving low-surface-brightness galaxies (LSBGs) including dwarf irregulars (see, e.g., Grebel 1999, 2000). Little is known about the census, formation conditions, and evolutionary status of the different types of XMPGs.

We have therefore begun a systematic search for XMPGs using the spectroscopic database of the Sloan Digital Sky Survey (SDSS). The SDSS (York et al. 2000) is an imaging and spectroscopic survey that will eventually cover about one quarter of the sky (more than 4000 deg^2 have been

imaged to date). After drift-scan imaging in five band-passes (Fukugita et al. 1996; Gunn et al. 1998; Hogg et al. 2001) photometry pipelines measure photometric and astrometric properties (Lupton et al. 2001; Stoughton et al. 2002; Smith et al. 2002; Pier et al. 2003) and identify candidate galaxies and quasars for multi-fibre spectroscopy. Each plate has 640 fibers, yielding 608 spectra of galaxies, quasars and stars and 32 sky spectra per pointing (Blanton et al. 2003). The fibers have a diameter of $3''$. The spectra cover a wavelength range of 3800 \AA to 9200 \AA with a resolution of ~ 1800 . The SDSS takes spectra of a magnitude-limited sample of galaxies (mainly field galaxies brighter than $r = 17^m77$; Strauss et al. 2002) and a color-selected sample of quasars (Richards et al. 2002). These include a substantial number of emission-line galaxies. The spectra are automatically reduced and wavelength- and flux-calibrated (see Stoughton et al. 2002; Abazajian et al. 2003, and <http://www.sdss.org/dr1/algorithms> for more details).

Owing to its homogeneity, area coverage, and depth, the SDSS provides an excellent means of creating a flux-limited sample of XMPGs. In this Letter we report the discovery of eight new XMPGs and the recovery of four previously known or suspected XMPGs. In Section 2 we briefly describe our analysis methods and the determination of oxygen abundances. In Section 3 we present our results and discuss them. In Section 3, our findings are summarized. Throughout the paper a Hubble constant of $H_0 = 75 \text{ km s}^{-1} \text{ Mpc}^{-1}$ is adopted.

¹ Max-Planck-Institut für Astronomie, Königstuhl 17, D-69117 Heidelberg, Germany; kniazev@mpia.de

² Princeton University Observatory, Peyton Hall, Princeton, NJ 08544-1001

³ Special Astrophysical Observatory, Nizhnij Arkhyz, Karachai-Circassia, 369167, Russia

⁴ Apache Point Observatory, P.O. Box 59, Sunspot, NM 88349

⁵ Institute for Cosmic Ray Research, University of Tokyo, 5-1-5 Kashiwa, Kashiwa City, Chiba 277-8582, Japan

2. SELECTION OF CANDIDATES AND CALCULATION OF OXYGEN ABUNDANCES

For our work we used reduced spectra from ~ 680 separate plates resulting in a total sample of $\sim 250,000$ objects with galaxy spectra. Approximately 10% of these plates were observed more than once, thus the above spectra also include galaxies with multiple observations. The total area on the sky covered by the analyzed SDSS spectroscopic database is ~ 3000 deg². For the analysis of the SDSS spectra we used our own software for emission-line data, which was created for the Hamburg/SAO Survey for Emission-Line Galaxies (HSS-ELG; Ugryumov et al. 2001, and references therein) and for the Hamburg/SAO Survey for Low Metallicity Galaxies (HSS-LM; Ugryumov et al. 2003). All emission lines were re-measured using a method detailed in Kniazev et al. (2000) and Pustilnik et al. (2002). The continuum was determined with the help of an algorithm described in detail by Shergin, Kniazev & Lipovetsky (1996).

We extracted a galaxy sample comprised only of objects with strong emission lines (rest frame $H\beta$ equivalent widths $EW(H\beta) \geq 20$ Å). Our selection procedure for galaxies with strong emission lines will be described in detail in Kniazev et al. (2003). Our $EW(H\beta)$ selection is motivated by the requirement to measure (1) the weak $[O\text{ III}] \lambda 4363$ Å emission line (whose intensity is usually $I_{4363} \leq 0.1I_{H\beta}$) for a direct calculation of the electron temperature, T_e , and (2) the $[O\text{ II}] \lambda 7319, 7330$ Å lines (usually $I_{7319+7330} \leq 0.05I_{H\beta}$) needed for the O^+/H^+ determination. These direct measurements tend to be possible only for spectra with sufficiently large Balmer emission equivalent widths.

While spectra obtained with fibre-fed spectrographs may be difficult to correct for atmospheric dispersion effects (Filippenko 1982), these problems are reduced for compact objects such as the $H\text{ II}$ regions in our target galaxies. We find this confirmed by the excellent agreement between our measured parameters and previously published values for already known XMPGs that we recovered from the SDSS data (see below). The SDSS spectra presented here were taken at airmasses of 1.18 ± 0.12 , which further reduces dispersion effects.

The abundances of the ionized species and the total oxygen abundance have been obtained with the method described by Izotov, Thuan & Lipovetsky (1994); Thuan, Izotov & Lipovetsky (1995), and Izotov & Thuan (1999), which was also used for the galaxies from the HSS-ELG and HSS-LM projects. The uncertainties of the measurements of line intensities, continua, extinction coefficients, and Balmer absorption equivalent widths have been propagated to derive the uncertainties of the element abundances. For objects with $z \leq 0.024$, the SDSS spectra do not include the $[O\text{ II}] \lambda 3727$ Å line, and hence the so-called “direct method” mentioned above cannot be used. Nor is it possible to use empirical R23 methods (Pagel et al. 1979; McCall, Rybski & Shields 1985; Pilyugin 2000, etc.), since all of them require the $[O\text{ II}] \lambda 3727$ Å line. However, as shown and tabulated by Aller (1984) for p^3 configurations, the measured intensities of the auroral lines $[O\text{ II}] \lambda 7319, 7330$ Å may be used instead to determine O^+/H^+ . The resulting O^+/H^+ values should be the same

with both methods, but since the total intensities of the $[O\text{ II}] \lambda 7319, 7330$ Å lines are much fainter than the $[O\text{ II}] \lambda 3727$ Å line, the application of the auroral line method is restricted to SDSS spectra with sufficiently high signal-to-noise ratio.

To test the accuracy of our abundance determinations we calculated oxygen abundances using both the $[O\text{ II}] \lambda 7319, 7330$ Å line method and the direct method for spectra with $z > 0.024$. In addition, we compared our results with those for galaxies in common with the studies quoted in the preceding paragraph. The published oxygen abundances of the famous XMPG I Zw 18 range from 7.05 to 7.2 in the northwest (NW) component along its major axis (see the Figure 5 from Izotov et al. 1999), and from 7.2 to 7.3 in the southeast (SE) component. Both of these components were targeted by SDSS spectroscopy, and our measured oxygen abundances agree within the cited uncertainties with the previous results (see Table 1). The oxygen abundance for HS 0822+3542 is 7.44 ± 0.06 according to Pustilnik et al. (2003) and is in excellent agreement with our value of 7.45 ± 0.02 . For HS 0837+4717, $12 + \log(O/H) = 7.64 \pm 0.04$ (Kniazev et al. 2000), which agrees with our SDSS abundance of 7.62 ± 0.02 calculated with the $[O\text{ II}] \lambda 3727$ Å line, and with our abundance of 7.63 ± 0.03 determined using the $[O\text{ II}] \lambda 7319, 7330$ Å lines. Finally, for our newly discovered XMPG SDSS J0519+0007 we find $12 + \log(O/H) = 7.46$ with either method, although the value obtained using $[O\text{ II}] \lambda 7319, 7330$ Å has a larger uncertainty. We conclude that SDSS spectra permit accurate oxygen abundance determinations over a studied range of $7.10 < 12 + \log(O/H) < 7.65$, and that the auroral line method appears to yield reliable results.

3. RESULTS AND DISCUSSION

Our survey led to the discovery of eight previously unknown XMPGs. In Figure 1 we show their SDSS spectra. Table 1 lists the properties of the new XMPGs as well as previously known XMPGs in the same area that were recovered by our programs and that have an abundance accuracy ≤ 0.1 dex. Column 1 gives the SDSS names derived from the J2000 coordinates of the fiber positions. Columns 2 and 3 contain the SDSS Petrosian integrated g and r magnitudes. Column 4 lists a preliminary morphological classification following KÖ00, column 5 SDSS redshifts z , column 6 oxygen abundances $12 + \log(O/H)$ with their uncertainties, and column 7 gives alternative galaxy names where available from the NASA/IPAC Extragalactic Database (NED). In Table 2 we present the corrected relative fluxes of lines used for the calculation of oxygen abundances, and their uncertainties.

In spite of three decades of searches for XMPGs, very few such objects are currently known. The new galaxies presented here increase the number of reliably known XMPGs by approximately one quarter, an important step in efforts to establish a comprehensive list of very metal-deficient galaxies with well-defined, uniform selection criteria and to study their group properties.

Our sample of new XMPGs contains the most distant and most luminous XMPG found so far (SDSS J0519+0007; $D \sim 177$ Mpc, $M_g \sim -18^m6$). SDSS J1215+5223, on the other hand, is one of the closest XMPGs if one simply converts its redshift into distance

(2.1 Mpc), although the caveat of peculiar velocities should be kept in mind for objects with distances of just a few Mpc (Karachentsev et al. 2002, 2003). The identification of very nearby XMPGs is of special importance since these objects permit detailed studies of their resolved star formation histories and of their overall age. The XMPGs found in the SDSS data cover a wide range of abundances (7.15 to 7.65), redshifts ($0.0005 < z < 0.0443$), and luminosities ($-12^m4 < M_g < -18^m6$). None of our new XMPGs is as metal-poor as I Zw 18 (which is among the XMPGs recovered in the SDSS data) or SBS 0335–052, which remain the most metal-deficient, star-forming galaxies known to date. XMPGs span at least 6 magnitudes in blue luminosity, suggesting possible atypical evolutionary histories for the most luminous objects, since they do not follow the “standard” luminosity-metallicity (L-Z) relation (see, e.g., Kunth & Östlin 2000). This is illustrated in Figure 2, where the new and the previously known XMPGs are plotted. While the LSBGs (primarily dwarf irregulars, dIrrs) tend to scatter around the L-Z relation previously measured for dIrrs (Skillman, Kennicutt & Hodge 1989; Richer & McCall 1995), most of the new and previously known very metal-deficient BCGs appear to be too luminous for their low present-day metallicities. Interestingly, the gas-deficient, quiescent dwarf spheroidal (dSph) galaxies would show the opposite trend if added to this plot: They appear subluminal for their low metallicity as compared to dIrrs (Grebel, Gallagher & Harbeck 2003, and references therein). These differences are not merely a bias introduced by the blue luminosity’s sensitivity to present-day activity; in fact, the immediate cessation of all star formation activity and subsequent passive fading would still require more than a Hubble time to erase the differences in luminosity (Grebel et al. 2003).

An interesting, yet controversial scenario is the possibility that XMPGs that clearly deviate from the L-Z relation are truly young galaxies, unenriched because they are now undergoing their first episodes of star formation. The nearest XMPGs for which detailed stellar population studies are available are all dIrrs within ~ 2 Mpc around the Local Group. They generally comply with the L-Z relation and contain old stellar populations (see Grebel 2000; Grebel, Gallagher & Harbeck 2003, and references therein). Deep HST imaging of nearby BCGs (typically at distances > 3 Mpc) shows that star formation has progressed for at least several Gyr (e.g., Dolphin et al. 2001; Izotov & Thuan 2002), but for more distant BCGs such as the famous I Zw 18, the age question remains unsolved (compare, e.g., Östlin 2000; Hunt, Thuan, & Izotov 2003). However, the older populations in I Zw 18 as well as in at least half of the new XMPGs of our sample should be resolvable with the Advanced Camera for Surveys aboard the Hubble Space

Telescope, which should allow us to settle the question of delayed star formation soon.

If BCGs underwent slow astration for most of their history, resulting in slow enrichment similar to that observed in dIrrs, and are now experiencing their first major starburst, then it is conceivable that this change in their mode of star formation was triggered by interactions with companion galaxies, or possibly primordial gas clouds. Alternatively, dwarf galaxies with particularly violent, bursty star formation episodes may suffer significant metal loss through winds from massive stars and supernova ejecta (e.g., Mac Low & Ferrara 1999). These different evolutionary scenarios result in predictions that can be tested via, for instance, optical, radio, and X-ray follow-up observations. An increased sample of XMPGs with well-defined, uniform selection criteria as provided by the SDSS is crucial for uncovering their individual and group properties.

By confining our search to galaxies with strong Balmer emission we ensure that we only include galaxies for which very accurate, direct oxygen abundance measurements based on the temperature-sensitive [O III] $\lambda 4363$ Å line and on the direct calculation of the electron temperature are possible. With these constraints, we find a surface density of XMPGs of ~ 4 per 1000 deg² for $r \leq 17^m77$ and $12 + \log(\text{O}/\text{H}) < 7.65$. Extrapolating to the full anticipated SDSS survey area, we expect to detect at least 20 additional galaxies once the SDSS is completed.

LH and MAS acknowledge the support of NSF grant AST-0071079.

Funding for the creation and distribution of the SDSS Archive has been provided by the Alfred P. Sloan Foundation, the Participating Institutions, the National Aeronautics and Space Administration, the National Science Foundation, the U.S. Department of Energy, the Japanese Monbukagakusho, and the Max Planck Society. The SDSS Web site is <http://www.sdss.org/>.

The SDSS is managed by the Astrophysical Research Consortium (ARC) for the Participating Institutions. The Participating Institutions are The University of Chicago, Fermilab, the Institute for Advanced Study, the Japan Participation Group, The Johns Hopkins University, Los Alamos National Laboratory, the Max-Planck-Institute for Astronomy (MPIA), the Max-Planck-Institute for Astrophysics (MPA), New Mexico State University, University of Pittsburgh, Princeton University, the United States Naval Observatory, and the University of Washington.

This research has made use of the NASA/IPAC Extragalactic Database (NED) which is operated by the Jet Propulsion Laboratory, California Institute of Technology, under contract with the National Aeronautics and Space Administration.

REFERENCES

- Abazajian et al. 2003, submitted (astro-ph/0305492)
 Aller, L.H. 1984, *Physics of Thermal Gaseous Nebulae*, Dordrecht: Reidel
 Blanton, M.R., Lupton, R.H., Maley, F.M., Young, N., Zehavi, I., & Loveday, J. 2003, *AJ*, 125, 2276
 Dolphin, A. E. et al. 2001, *MNRAS*, 324, 249
 Filippenko, A.V. 1982, *PASP*, 94, 715
 Fukugita, M., Ichikawa, T., Gunn, J.E., Doi, M., Shimasaku, K., & Schneider, D.P. 1996, *AJ*, 111, 1748
 Grebel, E.K. 1999, in *IAU Symp. 192, The Stellar Content of the Local Group*, ed. P. Whitelock & R. Cannon (Provo: ASP), 17
 Grebel, E.K. 2000, in *Star Formation from the Small to the Large Scale*, ESA SP-445, ed. F. Favata, A.A. Kaas, & A. Wilson (Noordwijk: ESA), 87
 Grebel, E.K., Gallagher, J.S., & Harbeck, D. 2003, *AJ*, 125, 1926
 Gunn, J.E. et al. 1998, *AJ*, 116, 3040
 Hogg, D.W., Finkbeiner, D.P., Schlegel, D.J., and Gunn, J.E. 2001, *AJ*, 122, 2129

- Hunt, L. K., Thuan, T. X., & Izotov, Y. I. 2003, *ApJ*, 588, 281
 Izotov, Y.I., Chaffee, F.H., Foltz, C.B., Green, R.F., Guseva, N.G., & Thuan, T.X. 1999, *ApJ*, 527, 757
 Izotov, Y.I., & Thuan, T.X. 1999, *ApJ*, 511, 639
 Izotov, Y.I., & Thuan, T.X. 2002, *ApJ*, 567, 875
 Izotov, Y.I., Thuan, T.X., & Lipovetsky, V.A. 1994, *ApJ*, 435, 647
 Karachentsev, I. D. et al. 2002, *A&A*, 389, 812
 Karachentsev, I. D. et al. 2003, *A&A*, 398, 479
 Kniazev, A.Y., Pustilnik, S.A., Ugryumov, A.V., & Kniazeva, T.F. 2000, *Astronomy Letters* 26, 129
 Kniazev, A.Y., Pustilnik, S.A., Pramsky, A.G., & Ugryumov, A.V. 2001, *A&A*, 371, 404
 Kniazev, A.Y. et al. 2003, in preparation.
 Kunth, D., & Östlin, G. 2000, *A&A Rev.*, 10, 1
 Lee, H., Grebel, E.K., & Hodge, P.W. 2003, *A&A*, 401, 141
 Lupton, R., Gunn, J.E., Ivezić, Z., Knapp, G.R., Kent, S., & Yasuda, N. 2001, in *Astronomical Data Analysis Software and Systems X*, ASP Conf. Ser. 238, eds. F. R. Harnden, Jr., F. A. Primini, & H. E. Payne (San Francisco: ASP), 269
 Mac Low, M.-M., & Ferrara, A. 1999, *ApJ*, 513, 142
 McCall, M.L., Rybski, P.M., & Shields, G.A. 1985, *ApJS*, 57, 1
 Östlin, G. 2000, *ApJ*, 535, L99
 Pagel, B.E.J., Edmunds, M.G., Blackwell, D.E., Chun, M.S., & Smith, G. 1979, *MNRAS*, 189, 95
 Pier, J.R., Munn, J.A., Hindsley, R.B., Hennessy, G.S., Kent, S.M., Lupton, R.H., & Ivezić, Ž. 2003, *AJ*, 125, 1559
 Pilyugin, L.S. 2000, *A&A*, 362, 325
 Pustilnik, S.A., Engels, D., Ugryumov, A.V., Lipovetsky, V.A., Hagen, H.-J., Kniazev, A.Y., Izotov, Y.I., & Richter, G. 1999, *A&AS*, 137, 299
 Pustilnik, S.A., Kniazev, A.Y., Masegosa, J., Márquez, I.M., Pramskij, A.G., & Ugryumov, A.V. 2002, *A&A*, 389, 779
 Pustilnik, S.A., Kniazev, A.Y., Pramsky, A.G., Ugryumov, A.V., & Masegosa, J. 2003b, *A&A*, submitted.
 Richards, G.T., Fan, X., Newberg, H.J., et al. 2002, 123, 2945
 Richer, M. G. & McCall, M. L. 1995, *ApJ*, 445, 642
 Salzer, J.J., Gronwall, C., Lipovetsky, V.A., et al. 2000, *AJ*, 120, 80
 Searle, L., & Sargent, W.L.W. 1972, *ApJ*, 173, 25
 Shergin, V.S., Kniazev, A.Yu., & Lipovetsky, V.A. 1996, *Astronomische Nachrichten*, 2, 95
 Skillman, E.D., Kennicutt, R.C., & Hodge, P.W. 1989, *ApJ*, 347, 875
 Skillman, E.D., Côté, S., & Miller, B.W. 2003, *AJ*, 125, 593
 Smith, J.A. et al. 2002, *AJ*, 123, 2121
 Stoughton, C. et al. 2002, *AJ*, 123, 485
 Strauss, M.A. et al. 2002, *AJ*, 124, 1810
 Terlevich, R., Melnick, J., Masegosa, J., Moles, M., & Copetti, M.V.F. 1991, *A&AS*, 91, 285
 Thuan, T.X., Izotov, Y.I., & Lipovetsky, V.A. 1995, *ApJ*, 445, 108
 Ugryumov, A. V., Engels, D., Kniazev, A. Y., et al. 2001, *A&A*, 374, 907
 Ugryumov, A.V., Engels, D., Pustilnik, S.A., Kniazev, A.Y., Pramsky, A.G., & Hagen, H.-J. 2003, *A&A*, 397, 463
 van Zee, L. 2000, *ApJ*, 543, L31
 York, D.G. et al. 2000, *AJ*, 120, 1579

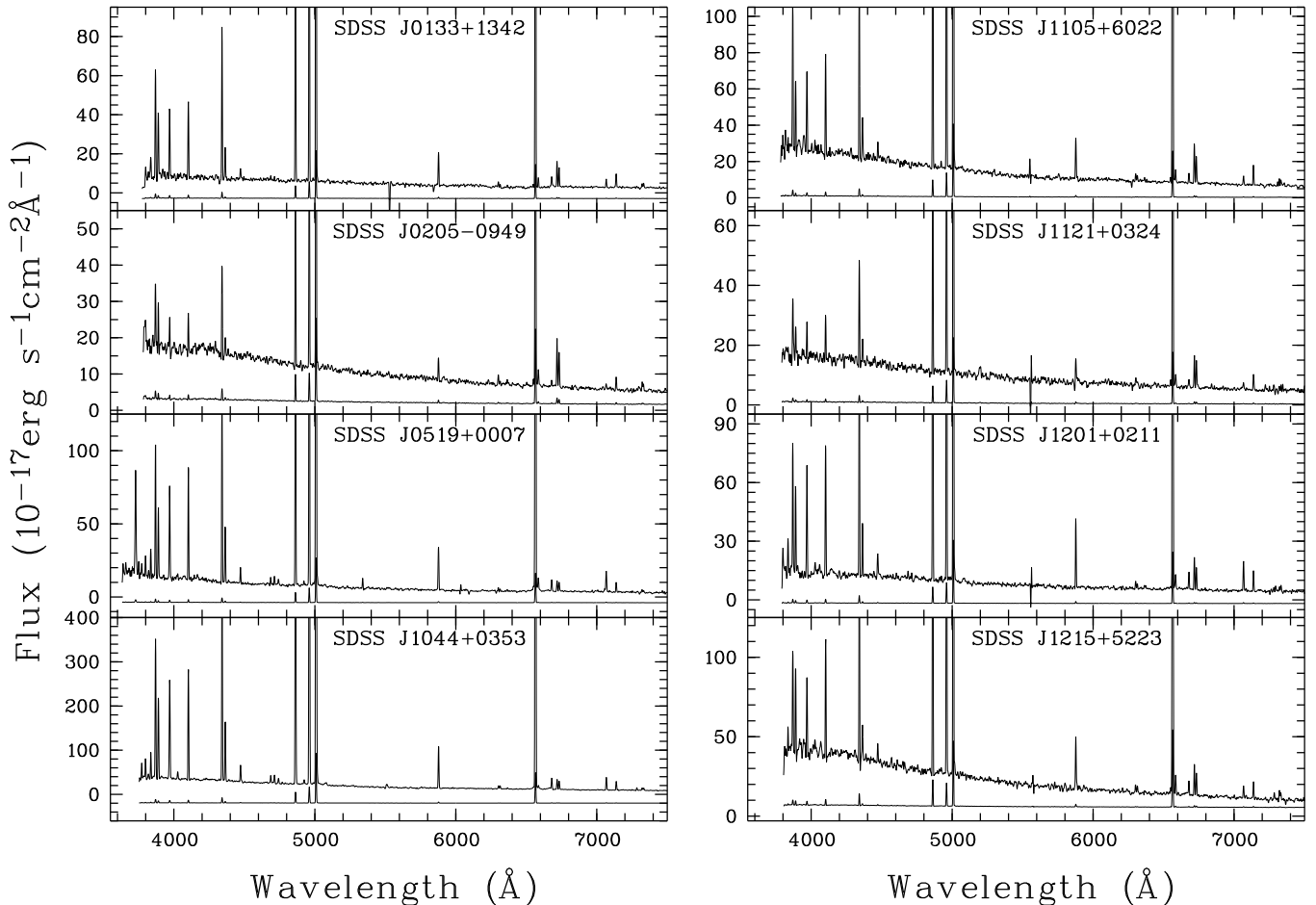


FIG. 1.— SDSS spectra of 8 new extremely metal-poor galaxies over the rest-frame wavelength range of 3600 Å to 7500 Å. The plot of the same spectrum in the bottom of each subpanel is scaled to visualize the ratios of the strongest emission lines.

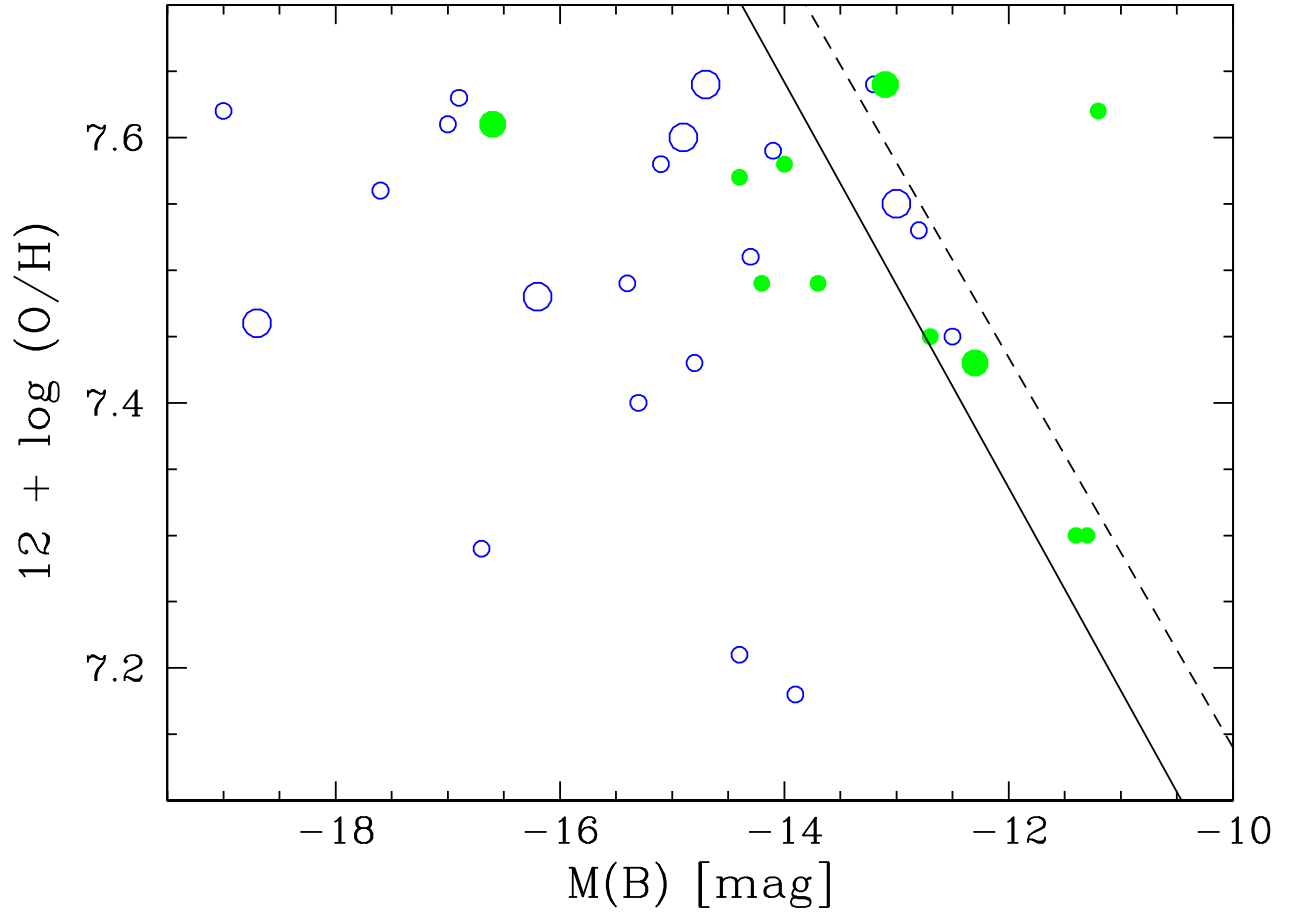


FIG. 2.— Blue luminosity versus oxygen abundance for previously known XMPGs with accurately measured oxygen abundances based on the direct method (small symbols; for references see Section 1), and for our new XMPGs (large symbols). Filled circles indicate LSBGs (mainly dIrrs). Open circles stand for BCGs. The diagonal lines indicate the luminosity-metallicity relation for dIrrs (solid line: Skillman et al. 1989; dashed line: Richer & McCall 1995). B -magnitudes were recalculated from SDSS g and r Petrosian magnitudes using equations from Smith et al. (2002).

TABLE 1

MAIN PARAMETERS OF THE NEW EXTREMELY METAL-POOR GALAXIES DISCOVERED IN THE SDSS, AND OF THE PREVIOUSLY KNOWN, RECOVERED ONES.

SDSS Name ^a	g^b	r	Type ^c	z	12+log(O/H)	Other names
(1)	(2)	(3)	(4)	(5)	(6)	(7)
SDSS J013352.56+134209.4	17.81	17.77	BCG	0.00867	7.60±0.03	
SDSS J020549.13−094918.1	15.27	15.10	LSBG	0.00643	7.61±0.09	KUG 0203−100
SDSS J051902.64+000730.0	18.29	19.23	BCG	0.04437	7.46±0.02	
SDSS J104457.84+035313.2	17.46	17.67	BCG	0.01279	7.48±0.01	
SDSS J110553.76+602228.9	16.37	16.32	BCG	0.00447	7.64±0.04	SBS 1102+606
SDSS J112152.80+032421.2	17.62	17.38	LSBG	0.00383	7.64±0.08	
SDSS J120122.32+021108.5	17.51	17.45	BCG	0.00329	7.55±0.03	APMUKS(BJ)
SDSS J121546.56+522313.9	15.75	15.87	LSBG	0.00052	7.43±0.06	CGCG 269−049
SDSS J082555.44+353231.9	17.74	17.76	BCG	0.00233	7.45±0.02	HS 0822+3542
SDSS J084030.00+470710.2	17.51	18.46	BCG	0.04203	7.62±0.02	HS 0837+4717
SDSS J093401.92+551427.9	16.03	16.06	BCG	0.00253	7.13±0.03	I Zw 18 (NW component)
SDSS J093402.40+551423.3	16.03	16.06	BCG	0.00259	7.25±0.04	I Zw 18 (SE component)
SDSS J111934.32+513012.2	16.81	16.79	BCG	0.00440	7.51±0.04	Arp dwarf, A1116+517

^aFollowing IAU conventions, the official SDSS designation for an object in the SDSS is SDSS JHH-MMSS.ss+DDMMSS.s, where the names consist of the J2000 coordinates of the source. Hereafter we are using in the text abbreviated names, SDSS JHHMM+DDMM.

^bSDSS Petrosian integrated magnitude

^cBCG stands for blue compact galaxy. LSBG denotes a low-surface-brightness galaxy.

TABLE 2

CORRECTED RELATIVE EMISSION LINE FLUXES AND ERRORS^a

Name	[O II] 3727 Å	H δ 4101 Å	H γ 4340 Å	[O III] 4363 Å	[O III] 4959 Å	[O III] 5007 Å	H α 6563 Å	[O III] 7319+7330 Å
(1)	(2)	(3)	(3)	(4)	(5)	(6)	(8)	(7)
SDSS J0133+1342	...	24.2±0.76	48.3±0.9	10.1±0.7	131.7±1.2	395.2±3.6	274.8±2.3	3.0±0.6
SDSS J0205−0949	...	24.9±3.69	48.8±2.8	7.3±1.5	99.4±1.9	294.6±4.6	276.9±4.7	5.4±1.2
SDSS J0519+0007	33.0±1.2	29.4±0.54	47.8±0.5	14.3±0.3	142.9±0.7	445.6±2.1	274.7±1.3	1.1±0.3
SDSS J1044+0353	...	25.7±0.28	48.0±0.4	13.6±0.2	142.4±1.2	443.9±3.8	274.6±1.7	1.1±0.2
SDSS J1105+6022	...	25.8±0.78	47.1±1.4	10.3±1.0	138.7±1.1	421.9±2.9	277.4±2.2	2.8±0.4
SDSS J1121+0324	...	26.9±2.68	47.1±2.7	8.5±1.6	124.7±2.6	352.0±6.1	278.0±5.1	4.6±1.1
SDSS J1201+0211	...	25.6±0.62	48.9±0.8	9.7±0.5	124.8±1.0	380.5±2.5	277.6±1.7	1.7±0.3
SDSS J1215+5223	...	25.0±1.49	47.6±1.4	6.3±0.9	84.5±0.8	236.2±2.0	277.0±2.6	3.1±0.4
SDSS J0825+3532	...	23.6±0.35	44.5±0.5	10.3±0.3	119.8±0.7	358.9±2.1	275.5±1.7	1.4±0.2
SDSS J0840+4707	45.4±0.9	27.9±0.43	46.9±0.6	17.0±0.4	190.3±1.4	577.3±4.2	275.3±2.1	2.2±0.1
SDSS J0934+5514	...	24.5±0.87	48.6±0.7	7.3±0.4	69.4±0.5	214.6±1.3	274.6±3.5	0.7±0.2
SDSS J0934+5514	...	24.4±0.52	48.4±0.6	4.7±0.4	55.7±0.4	182.4±1.2	276.8±1.3	1.4±0.2
SDSS J1119+5130	...	23.2±2.05	49.0±1.5	7.2±0.7	96.9±1.0	281.3±2.6	276.6±2.5	2.9±0.5

^aWe show corrected flux ratios $100 \cdot I(\lambda)/I(H\beta)$